Influence of machining parameters on microdrill performance

G. Hemanth and G.L. Samuel*

Department of Mechanical Engineering,
Indian Institute of Technology Madras,
Chennai 600036, India
Fax: +91-44-2257-4652
E-mail: hemanth@inphinity.co.in
E-mail: samuelgl@iitm.ac.in
*Corresponding author

N.J. Vasa

Department of Engineering Design,
Indian Institute of Technology Madras,
Chennai 600036, India
E-mail: njvasa@iitm.ac.in

Abstract: There is an increasing interest in microdrilling of metallic and other miniaturised components. Drill breakage is the most prevalent problem with microdrill that possesses high length-to-diameter ratio. In this paper, finite element modelling approach is used to determine the buckling load of a microdrill while drilling metallic components. The influence of variation in flute length, diameter, helix angle and lip angle on buckling load during machining of metallic components is studied. Empirical loading equation based on the material hardness, feed and diameter of the microdrill is also used to estimate the loading condition during microdrilling operation. Results are in agreement with the buckling loads predicted by proposed finite element model. In the present work emphasis is made on estimating the critical feed and the speed based on modal analysis while machining various materials. Tool failure can be avoided by maintaining the machining conditions within these critical operating parameters.

Keywords: microdrilling; Euler buckling load analysis; critical feed; finite element model.

Reference to this paper should be made as follows: Hemanth, G., Samuel, G.L. and Vasa, N.J. (2011) 'Influence of machining parameters on microdrill performance', *Int. J. Manufacturing Technology and Management*, Vol. 22, No. 2, pp.124–144.

Biographical notes: G. Hemanth received his Bachelor of Technology in Mechanical Engineering at Indian Institute of Technology Madras in the year 2008. His areas of interest include computer aided manufacturing, micro machining, and metrology.

G.L. Samuel is currently working as an Assistant Professor at the Department of Mechanical Engineering, Indian Institute of Technology Madras, Chennai. He received his BE in Mechanical Engineering from Mysore University in

1991, MTech in Production Engineering and Systems Technology from Kuvempu University in 1994 and PhD in Mechanical Engineering from Indian Institute of Technology Madras in 2001. He has been a Post Doctoral Fellow at School of Mechanical Engineering, Kyungpook National University, South Korea. His active areas of research are: measurements and inspection of freeform surfaces, geometric error compensation in machine tools, and evaluation of form errors, micromachining and laser vision systems. He has published over fifteen papers in refereed international journals.

Nilesh J. Vasa received his BE in Production Engineering (Bombay University, India), MTech in Mechanical Engineering (IIT Madras, India) and Doctorate of Engineering in Electronic Device Engineering (Kyushu University, Japan) in the year 1988, 1990 and 1997, respectively. He worked as a faculty member at Kyushu University, Japan until 2005. Currently, he is a faculty member at IIT Madras, India. His current research areas include micro-manufacturing, laser assisted sensing, laser assisted manufacturing, and opto-mechatronics devices. He is a member of SPIE, OSA, Indian Laser Association and Laser Society of Japan.

1 Introduction

In recent years, with the advancement in manufacturing technology, the production of miniaturised components down to the size of few micrometers is common for various applications. Micromanufacturing gains importance mainly from two requirements: greater compactness in the utilisation of space and portability. Different types of mechanical micromachining processes include microdrilling, microturning, micromilling etc. The machines that manufacture these items need to be produced in ever decreasing sizes, with tightly specified dimensions and accuracies. The term 'micromachining' has thus emerged and is generally used to define the practice of material removal for the production of parts having dimensions that lie between one and 999 μm, although, an upper limit of 500 μm has been considered to set the border between the micro- and the macromachining (Mahalik, 2006).

Microdrilling plays an important role in modern industry, especially in electronics industry for the machining of printed circuit boards (PCB), manufacturing of air bearings and bushings, EDM tooling, nozzles, microwave components, gas and liquid flow, medical equipment, optical components etc. Drilling in the micro ranges, using the special microdrills, requires precision microdrilling equipment (Joseph, 2002). Various microdrilling methods have been introduced such as laser microdrilling, electrochemical, ion and electron beam microdrilling, electrical discharge machining (EDM) apart from the mechanical microdrilling process. But, the machining accuracy of the EDM method is limited by tool wear, which is unavoidable consequence in an EDM process because the sparks generated for the machining remove the part of the tool electrode simultaneously. Therefore, both the depth and the shape control of the machined hole are critical requirements. Another microdrilling technique is by utilising the phenomenon of ultrafast pulse laser interference. 300 nm holes were successfully drilled on a 0.1 μm thick gold film using the laser beam. The major problem of laser microdrilling is that the process has a short focal depth. The beam undergoes diffraction and spreads out resulting in a

shift of focal depth. On the other hand, in order to produce holes with high slenderness ratio and geometrical accuracies, mechanical microdrilling is suitable process.

Though many aspects of microdrilling and macrodrilling have fundamentally identical features, the downsizing of drill bit dimensions introduces an array of problems, which produce a profound influence on the microdrilling process. The problems include highly reduced mechanical strength, effects of relatively larger web thickness, unavoidable drill deflections in the hole and the resulting interactions with the hole. The major differences exist between the microdrill and macrodrill in their geometry and their mode of failure. The microdrills have a larger shank diameter, which facilitates proper holding of the drill bit in the spindle unlike in macrodrill where the shank and the flute have the same diameter. The lip angle is often increased in microdrill to increase the strength at the chisel edge. A lip angle of 118° to 135° is used for microdrills whereas it is around 108° in case of macrodrill. To increase the strength of the flutes, the web thickness is increased (Hinds and Treanor, 2000). Microdrills usually have a high length to diameter ratio, i.e., holes lesser than 0.5 mm in diameter with aspect ratio more than ten. Larger aspect ratio results in buckling of drills. Due to buckling, drill hole widens and drill deviates from its axis and ultimately leads to drill breakage. Microdrills are typically made up of either cobalt steel or micro grain tungsten carbide. The steel drills are less expensive and easier to grind but are not as hard or as strong as the tungsten carbide drills. The drill point angle is based on the material to be drilled. The normal point angle is 118° and 135° is used for hard materials. The larger included point angle provides more strength at the drill point. Due to its size and shape, microdrills need to be used with care in order to drill holes accurately and to prevent drill failure.

To ensure productivity, quality, and safety, detection of microdrill breakage is important. The microdrills need to be used with care in order to drill holes accurately and to prevent drill breakage. The drills must be operated with restricted operating parameters and the drills of the correct geometry be used for a given operation. Generally, the drill breakage occurs due to excessive thrust force or torque on the drill bit. This is evident by examining the fractured surface of a drill, which will show a different characteristic depending on the type of excessive stresses that caused breakage. The microdrills suffer more than drills of larger diameter from drill breakage; the macrodrills generally fail due to wear out, long before the breakage occurs (Fu et al., 2007). It is also been indicated by examining the fracture surface that the tungsten carbide microdrills fail due to brittle fracture (Jeong and Min, 2007)

The drill point geometry defined by the shapes of the flute and flank surfaces is a primary factor to be considered when attempting to improve the machining performance of the drill (Sedat, 2007; Jung, 2005). There has been a great deal of work on microdrill geometry and drill cutting mechanics, the problems of producing and optimising drill geometry in microdrills still a challenge. The physical size of the tool limits the choice of the type of point geometry that can be employed. Other geometric features must be adjusted to maintain as much material as possible for extra strength and rigidity. The major difficulties in microdrilling are related to the wandering motions during the initial phase, high aspect ratios, high temperature etc. (Chyan and Ehmann, 1998; Cheong et al., 1999). However, of all the problems, the most undesirable ones are the increase in the cutting forces as the drill penetrates deeper into the hole. This is mainly caused by the chip related effects. As the chip moves along the flute of the drill bit, the friction between the chip and the drill flute increase the total torque that is acting on the drill bit

(Yongping et al., 2003). The low rigidity of the drill bit often leads to drill failure due to the excessive cutting force.

Chen and Ehmann (1994) followed an experimental approach for analysing the performance of the microdrill. Strenkowski et al. (2004) proposed an analytical finite element model for predicting thrust force and torque of generic macrodrills. Rahman et al. (2009) studied the effect of drilling parameter such as spindle speed, feed rate and drilling tool size on material removal rate (MRR), surface roughness, dimensional accuracy of brass material. Correlation between the radial run-out of drills and the hole quality was examined experimentally for microdrilling of PCBs (Watanabe et al., 2008). Peck drilling method is proposed for deep micro hole drilling of steels (Kim et al., 2009). In this method, microdrill utilises an intermittent feed and one and a half times longer than the conventional drill diameter.

It is observed from the literature that the tool breakage depends on the drill geometry. In the present work, the influence of variation in flute length, diameter, helix angle and lip angle on buckling load, particularly, during machining of metallic components is studied. Influence of various machining and geometrical parameters of typical microdrills on the buckling load is analysed based on finite element modelling. A drill bit with a typical geometry is modelled using PRO-E and the stress analysis is carried out using ANSYS for the given loading condition. To estimate the critical speed and critical feed for machining various materials, an empirical analysis as well as a finite element approach is used. In addition, modal analysis has been carried out to estimate the critical speed and to avoid wandering of micro tool.

2 Finite element modelling and analysis of microdrill

2.1 Element model

When microdrill is subjected an axial drilling force, it bends and deforms elastically in radial and axial directions. Timoshenko beam theory and shaft element is used for developing the finite element model of the microdrill. The shaft element of length L bends due to the axial drilling force P. The element has potential energy of the bending, shear potential energy from shear deformation caused by bending and energy produced by the axial forces P (Strenkowski et al., 2004). These energies and their sum can be expressed as equation (1)

$$U = \frac{1}{2}\int_0^L EI(\theta'^2_x + \theta'^2_y)dS + \frac{1}{2}\int_0^L kGA(x'^2_s + y'^2_s)dS - \frac{1}{2}\int_0^L P(x'^2 + y'^2)dS \tag{1}$$

where

E Young's modulus

I moment of inertia

k Poisson's ratio

G shear modulus

A area of cross-section

P axial load

x' denotes partial differentiation with respect to s.

The element is turning through constant speed and displaces due to bending. Hence, the element has kinetic energies produced within and it is given by (2)

$$T = \frac{1}{2}\int_0^L \rho A(x'^2 + y'^2)dS + \frac{1}{2}\int_0^L I(\theta'_x{}^2 + \theta'_y{}^2)dS + \frac{1}{2}\int_0^L I_p\omega^2 dS + \frac{1}{2}\int_0^L I_p\omega(-\theta'_y\theta_x + \theta'_x\theta_y)dS \tag{2}$$

where

ρ density

I_p polar moment of inertia

ω angular velocity

θ_x, θ_y angular displacements in x and y directions.

Displacements at any position of an element can be expressed approximately by the generalised displacements of nodes and the shape functions as:

$$\begin{aligned} x &= \{N\}\{q_u\} \\ y &= \{N\}\{q_v\} \\ -\theta_x &= \{N\theta\}\{q_v\} \\ \theta_y &= \{N\theta\}\{q_u\} \end{aligned} \tag{3}$$

where $\{q_u\}$, $\{q_v\}$ are the displacement vectors of the nodes

The generalised displacements and forces of the drilling system are expressed in complex form to analyse easily as:

$$\begin{aligned} &[M]\{Z''\} - i\omega[C][Z'] - ([K] - P[K_P])\{Z\} = \omega^2\{Q\}e^{i\omega t} \\ &\{Z\} = \{A\}e^{i\omega t} \end{aligned} \tag{4}$$

where $\{A\}$ is the amplitude vector of deformation at any position in the drilling system and is expressed as follows:

$$\{A\} = \omega^2\left[\omega^2(-[M] + [C]) + ([K] - P[K_P])\right]^{-1}\{Q\} \tag{5}$$

Directly assembling these element matrices, the general forms of the global system of equations (Sunil, 2007; Gurkan and Mustafa, 2004) are obtained as given below;

$$Mq'' + Cq' + (K_B + K_F + K_W)q = 0 \tag{6}$$

where M, K_B, K_F, K_W are the symmetric mass and stiffness matrices; the matrix C is the skew symmetric Coriolis matrix, K_B is the element stiffness matrix due to the bending and shear effects; K_F is the element stiffness matrix due to the axial force; K_W being the stiffness matrix due to the rotational speed or the inertia effects.

A non-trivial solution for the equation (6) is sought which reduces the system to the following set of equations (Pei et al., 2006).

The eigenvalue equation to analyse the buckling load is written as follows:

$$(K_B + K_W)q = (-K_F)q = F[F]q \quad \text{or} \quad \left[K_B + K_W - F[F]\right][q] = 0 \tag{7}$$

where F is the value of the critical buckling load.

The case $\omega = 0$ relates to the static buckling problem and hence gives the buckling load at the static loading condition

The eigenvalue equation to analyse the critical speed is written as:

$$(K_B + K_F)(q) = \omega^2 \left[\overline{M}\right] \quad \text{or} \quad K_B + K_F - \omega^2 \left[\overline{M}\right] = 0 \tag{8}$$

The case $F = 0$ relates to the zero loading condition.

The analytical results for the drill bits are obtained using Euler buckling formulae and are compared with the results obtained through finite element method. The buckling formula for the Euler-Bernouilli beam is given as follows:

$$P_{EU} = \pi^2 EI / (kl)^2$$

where P_{EU} is the Euler buckling load, E is young's modulus, I is area moment of inertia along the cross-section, k is a constant dependent on the boundary condition and l is the flute length of the drill bit

Figure 1 Typical geometry of microdrill (see online version for colours)

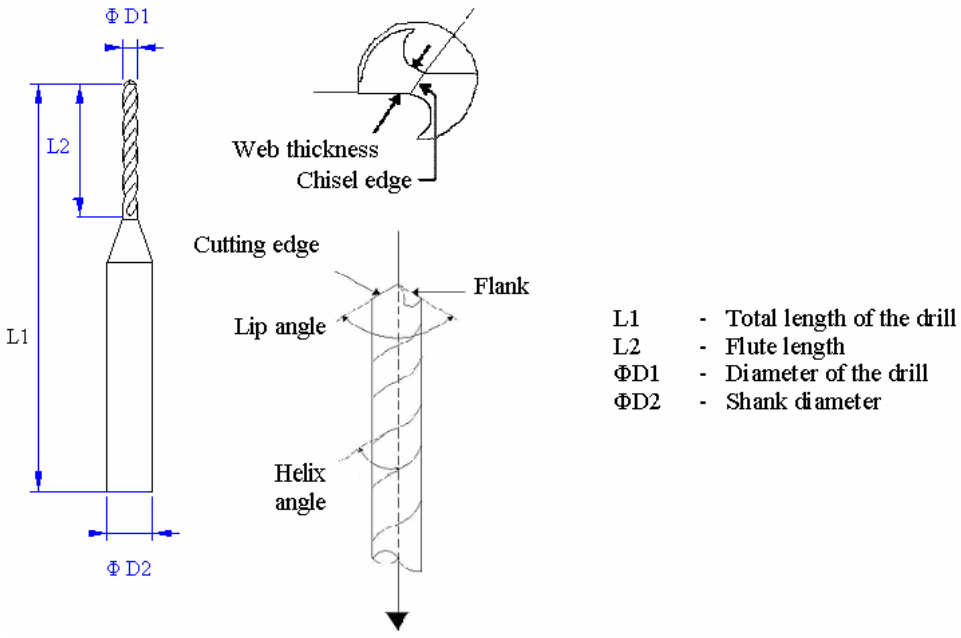

Figure 2 3D model of a microdrill bit (see online version for colours)

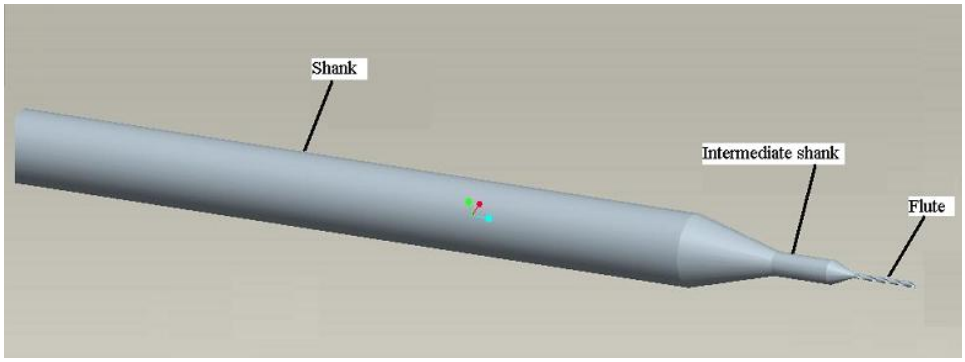

Figure 3 Element solid ten node 92 in ANSYS (a) element model (b) meshing of microdrill (see online version for colours)

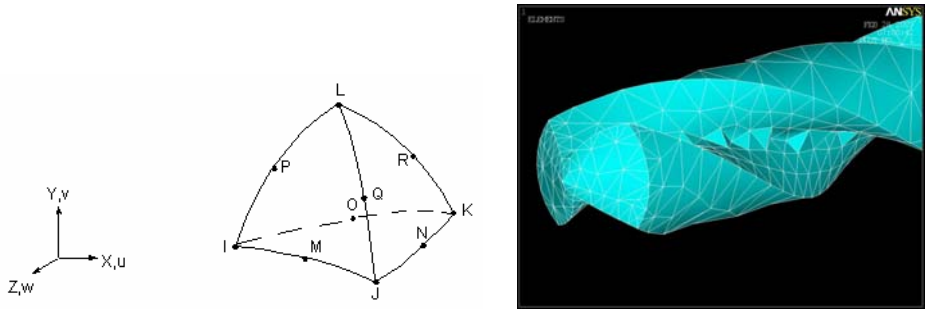

(a) (b)

2.2 *Finite element model and analysis*

Generally, the drill bit is modelled as a long twisted beam (Pei et al., 2006; Sunil, 2007). In the present work, the typical dimensions of the microdrill geometric parameters such as total length of drill, helix angle, lip angle and diameter are selected based on the models proposed in the literature. Figure 1 shows the geometric details of the typical microdrill.

The drill bit is modelled in PRO-E, a three dimensional modelling software and is then imported to ANSYS, a finite element software.

In the present analysis, high speed steel (HSS) is chosen as the material for microdrill with Young's modulus (E) of 200 GPa, density 8 kg/cm3 and Poisson's ratio as 0.27. A ten node tetrahedral structural solid element as shown in Figure 3(a) is chosen for meshing from the given element library. The element is defined by ten nodes having three degrees of freedom at each node: translations in nodal x, y and z directions.

Figure 3 (b) shows the microdrill meshed using the solid element in ANSYS. The stress analysis is performed on the model under a given loading condition and the stress isograms are obtained. The input parameters for stress analysis are given in Table 1.

Thrust force and the torque to be applied on the chisel edge and the cutting edges are calculated using equations (9) and (10) respectively as suggested by Sedat (2007). It is assumed that the thrust force and torque acts uniformly along the edges.

$$T = 12.501\, H_b \times f^{0.8} \times d^{0.8} - 0.041\, H_b \times d^2 \tag{9}$$

$$M = 0.00377 H_b \times f^{0.8} \times d^{1.8} \tag{10}$$

where T is the thrust force (N), H_b is Brinell hardness, f is the feed in mm/rev, d is the diameter in mm and M is the torque (N/mm).

Table 1 Input parameters for stress analysis

S. no.	*Description of items*	*Input*
1	Drill material	HSS
2	Workpiece materials	EN AW 2017 aluminium alloy; H_b = 931 N/mm^2
3	Drill geometry	Diameter = 0.1 mm, body length = 1mm
		Lip angle = 118° , flute length = 1 mm
		Helix angle = 30°
4	Element geometry	Ten node tetrahedral element (ANSYS solid 10 node 92); size = 0.01 mm
5	Process parameters	Spindle speed = 20,000 rpm; feed = 0.026 m/sec
	Loads	Thrust force = 0.56 N; torque = 0.15 N-mm

2.3 Determination of buckling load

Buckling is a failure mode characterised by a sudden failure of a structural member that is subjected to high compressive stresses where the actual compressive stresses at failure are smaller than the ultimate compressive stresses that the material is capable of withstanding. Mathematical analysis of buckling makes use of an eccentricity that introduces a moment which does not form part of the primary forces to which the member is subjected. Buckling load is the load at which certain types of structures become unstable and the displacement curve of the column deviates from linearity and the structure fails. Each load has an associated buckling mode shape; this is the shape that the structure assumes in a buckling condition.

In the present work, the eigenvalue analysis is carried out for determining the buckling load in the microdrill bits. Eigenvalue analysis predicts the theoretical buckling strength of an ideal elastic structure. It computes the structural eigenvalues for the given system loading and constraints. This is known as classical Euler buckling analysis.

For the buckling analysis, the meshing is done similar to that in the stress analysis. The type of element and the material properties are defined and a non-uniform meshing is done with the appropriate element size. To perform the eigenvalue buckling analysis, pre-stress effects are activated and the boundary conditions are applied. All degrees of freedom for the shank and the chisel edge of the drill are restricted. A load of 1 N is applied axially into the drill at the drill point. The 'Block Lanczos' method is used as the extraction method. This method is used for symmetric eigenvalue problems and uses sparse matrix solver. When the system is solved for this load step, the displacement curve

for the drill at the buckling is obtained. The buckling load is displayed as a factor multiplied by the applied load (i.e., 1 N). Drill bits of various geometries are made in PRO-E with varying diameters in steps of 0.1 mm while other geometric parameters remain constant. Similarly, the flute length is varied in steps of 0.5 mm. The variation of the buckling loads and the critical speeds with helix angle and lip angle is also studied. Table 2 shows the results for the computation time for the various grade of microdrill bit in the present analysis.

Table 2 Convergence of results with element size

Grade	*Buckling load (N)*	*Computation time taken for the of the stiffness matrices (min)*
5	0.560	13.0
6	0.556	6.0
7	0.558	2.5
8	0.546	1.5
9	0.537	1.0
10	0.517	1.0

2.4 Determination of critical feed

In order to avoid drill breakage, the feed given to the drill bit must be restricted. The thrust force which is dependent on the feed apart from the workpiece material and the diameter of the drill bit must not exceed this buckling load. Once the thrust force exceeds this buckling load, the displacement curve of the drill bit deviates from linearity and the drill is said to be failed. Eventually on increasing the thrust force to a greater amount, the drill breaks. Drill breakage is the most prevalent problem with microdrill. Hence, by limiting within this critical feed, the drill failure can be avoided. Thrust force and torque acting on micro-drill are estimated based on equations (9) and (10) as suggested by Sedat (2007).

3 Results and discussions

3.1 Stress analysis on cutting edge and chisel edge

The thrust force and the torque are applied to the chisel edge and the cutting edges of microdrill for the values obtained using equations (9) and (10). Stress isograms for various conditions and the contour plots are obtained using ANSYS. The contour plots for first, second and third principal stresses, and the Von Mises stresses are presented in Figure 4. From the analysis of the stress plots, it is seen that there is higher stress concentration at points on chisel edge and cutting edge and maximum values being at the points, which overlap both the regions. Results obtained using FE model were qualitatively in agreement with stress distribution in drill bits while machining of PCBs reported by Hinds and Treanor (2000).

Figure 4 Stress distribution on cutting edge and chisel edge (a) first principal stresses (b) second principal stresses (c) third principal stresses (d) Von Mises stresses (see online version for colours)

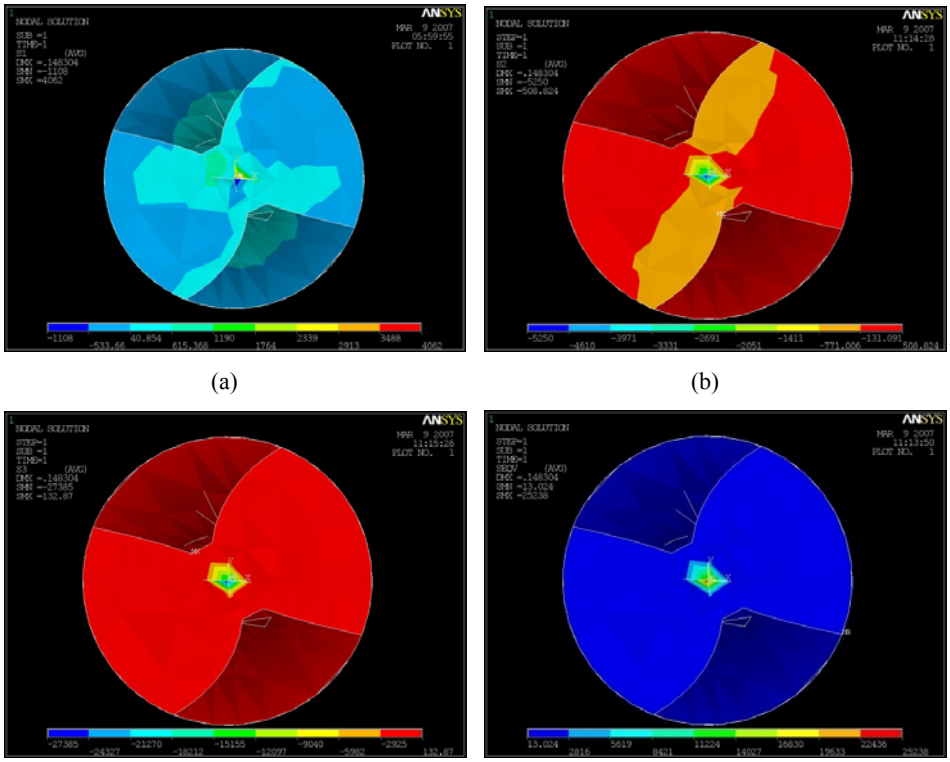

(a) (b)

(c) (d)

3.2 Validation of proposed FE model

In order to validate the model, the buckling results obtained using the finite element analysis in ANSYS is compared with those obtained using Euler formula. The comparison of these results are given in Table 3 and plotted for different tool diameters as shown in Figure 5. It is seen that the buckling loads obtained through the finite element analysis are in agreement with the buckling loads obtained through the Euler buckling formulae for an Euler-Bernouilli beam.

From Figure 5, it is observed that the increase in drill bit diameter increases the buckling load of microdrill bit. Buckling load analysis is carried out for different length of drill bits with 0.5 diameter and 30° helix angle using the proposed FE model and compared with analytical Euler formula. The buckling load a drill bit can withstand decreased with increase in the flute length of the drills. Similar trend is observed in the values of buckling load determined using Euler formula and the results are tabulated in Table 4 and presented graphically in Figure 6. Results based on FE model for microdrilling in metallic components are qualitatively in agreement with that of reported by Chen (2007) for PCB components. With these confirmatory results, further analysis is

carried out to establish buckling loads for different conditions and to determine the critical feed while carrying out microdrilling.

Table 3 Effect of drill diameter on buckling load

S. no.	*Drill bit diameter (mm)*	*Buckling load (N)*	
		Euler formula (P_{EU})	*Proposed FE model (P_{cr})*
1	0.1	0.67	0.79
2	0.2	2.68	3.10
3	0.3	6.08	7.07
4	0.4	10.9	11.46
5	0.5	16.77	15.73

Figure 5 Buckling load analysis for different diameter drill bits (see online version for colours)

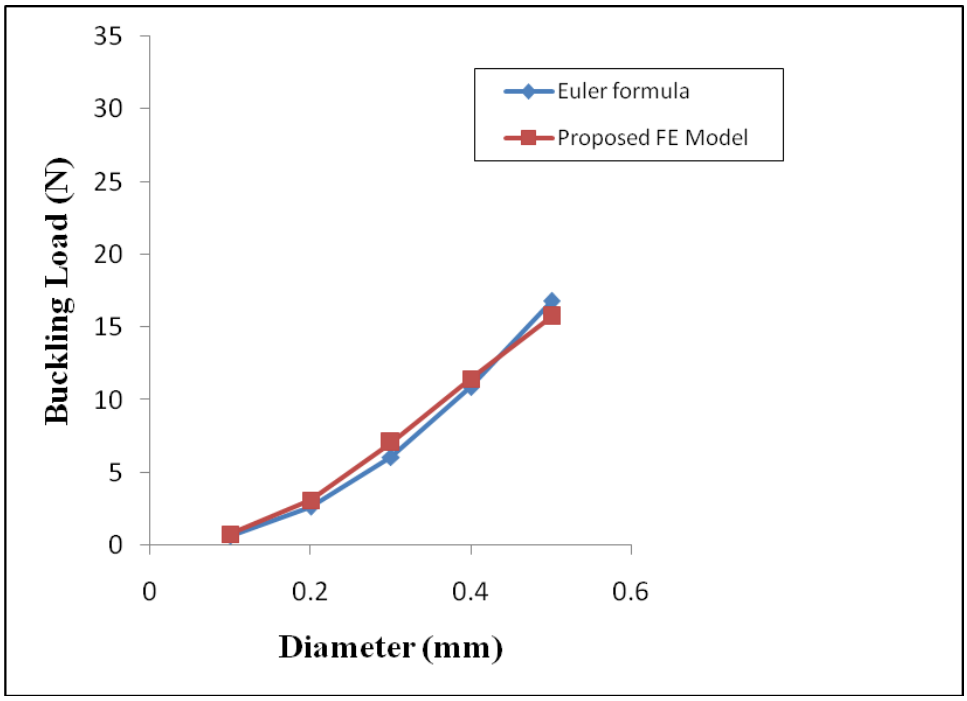

Table 4 Effect of flute length on buckling load with 0.5 diameter and 30° helix angle

S. no.	*Flute length (mm)*	*Buckling load (N)*	
		Euler formula (P_{EU})	*Proposed FE model (P_{cr})*
1	5	32.8	31.45
2	5.5	27.16	26.13
3	6	22.8	22.16
4	6.5	19.45	18.46
5	7.0	16.77	15.73

Figure 6 Buckling load analysis for different flute lengths (see online version for colours)

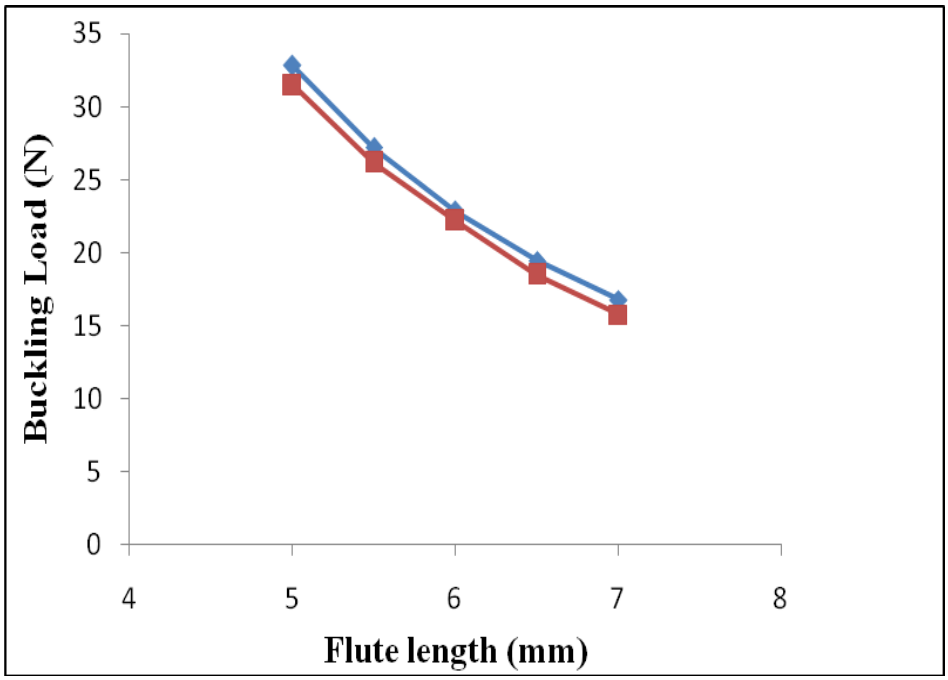

Figure 7 Results of buckling load analysis (see online version for colours)

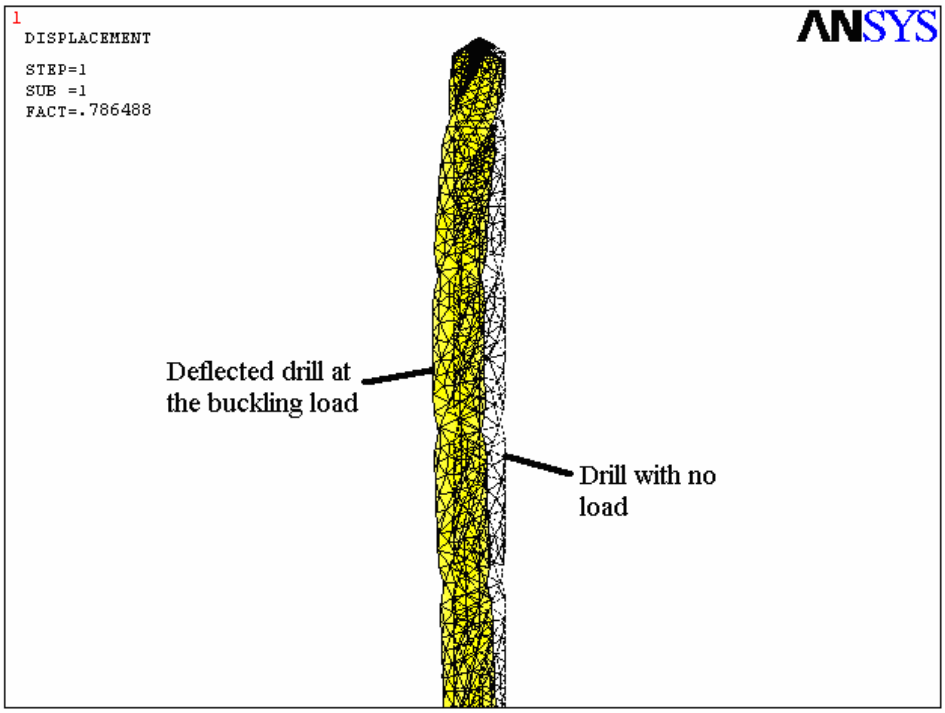

3.3 Determination of buckling load and critical feed

Drill bits with different geometries were modelled using PRO-E and the analysis is carried out using ANSYS. The results of buckling load for various cases are determined using proposed FE model by varying different geometric parameters. Different workpiece materials are considered for modelling the drill bits and the variation of their critical feeds with the drill geometry is studied. The materials considered are aluminium (95 BHN), carbon steel (180 BHN), stainless steel (200 BHN) and alloy steel (370 BHN). Figure 7 shows a graphical view of displacement of elements and nodes of a tool of 0.1 mm diameter for the critical buckling loads. It may be noted that the displacement curves plotted in Figure 7 have been scaled up for better visualisation. The critical feeds are estimated based on the buckling load for different materials. The critical feed in the present work are given in mm/rev. However, in practice the feed rate can be estimated in mm/sec based on the rotational speed of the spindle.

3.3.1 Variation with diameter

The buckling load and the critical feeds for the microdrills were obtained for different tool material and drill diameters and the results are presented in Table 5. It can be seen that the buckling load increases with the increase in diameter while other geometric parameters are kept constant.

Figure 8 presents the plot of variation of critical feed with diameter of the drills. The critical feed rates are higher when the diameter of the tool is increased. While machining the feed rates can be higher even for tools with lower diameter. However, while machining hard materials like steels, the feed rate has to be lower to avoid breakage of tools. If the feed rates are beyond the critical feeds, the stresses in the tool will be higher and the drill bit will break.

Figure 8 Effect of drill diameter on the critical feed for different workpiece materials (see online version for colours)

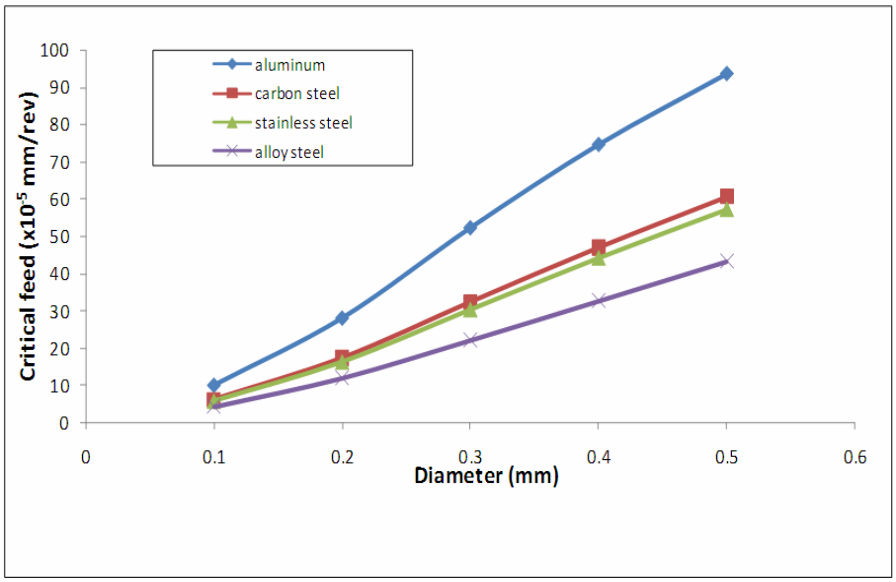

Table 5 Estimated buckling loads and critical feeds for different tool materials of varying drill diameters

S. no.	*Diameter (mm)*	*Buckling load (N)*	*Critical feeds (10^{-5} mm/rev)*			
		Proposed FE model (P_{cr})	*Aluminium*	*Carbon Steel*	*Stainless steel*	*alloy steel*
1	0.1	0.79	10.1	6.25	5.84	4.23
2	0.2	3.10	28.1	17.4	16.3	11.9
3	0.3	7.07	52.3	32.4	30.3	22.0
4	0.4	11.46	74.6	47.0	44.1	32.5
5	0.5	15.73	93.6	60.6	57.1	43.1

3.3.2 Variation with length

The length of the tool is an important factor in microdrilling. Generally, the microdrilling using drill bits is limited by the length of the tools. It is difficult to drill deep holes and through holes in thick materials. Buckling load and critical feed analysis is carried out for different flute length for microdrill bit of diameter 0.5 mm and the results are presented in Table 6. It is observed that the buckling load of the tools will decrease significantly as the flute length of the tool increases.

From Figure 9, it is seen that the critical feed rates that can be used while machining different materials also decreases with increase in flute length. Due to this trend the microdrills having a very high length to diameter ratio suffer commonly from tool breakage.

Table 6 Estimated buckling loads and critical feeds for different work materials with tool of varying flute lengths

S. no.	*Flute length (mm)*	*Buckling load (N)*	*Critical feeds (10^{-5} mm/rev)*			
		Proposed FE model (P_{cr})	*Aluminium*	*Carbon steel*	*Stainless steel*	*alloy steel*
1	5.0	31.5	171.6	97.8	90.1	59.7
2	5.5	26.1	144.2	84.8	78.6	54
3	6.0	22.2	124.5	75.4	70.3	49.8
4	6.5	18.5	106.6	66.9	62.7	45.9
5	7.0	15.7	93.7	60.7	57.2	43.1

3.3.3 Variation with helix angle

To study the influence of the helix angle on the performance of the tool, the helix angle is varied from 200 to 500 keeping the diameter and flute length constant and the buckling load and critical feeds are estimated. From the Table 7 and Figure 10, it is observed that the influence of the helix angle on the buckling load is very insignificant compared to the influence of other geometric parameters of the microdrills. It is found that the critical feed is not influenced much by the helix angle as observed from Table 7 and Figure 11.

Figure 9 Variation of critical feed with flute length for different work materials (see online version for colours)

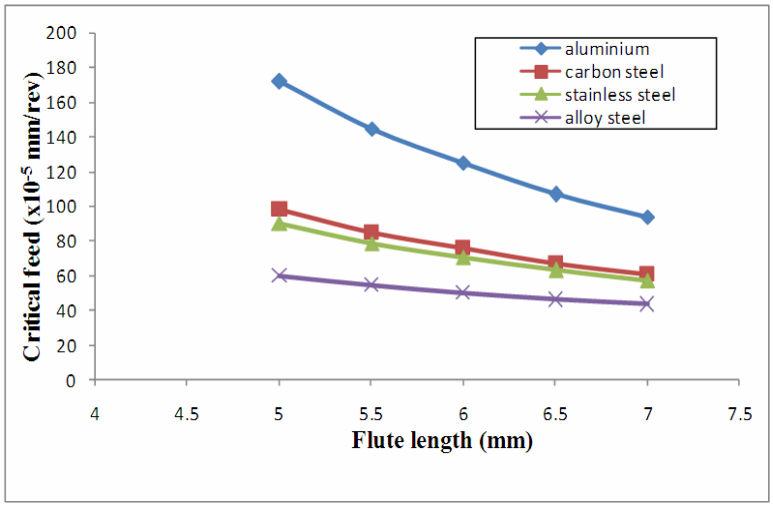

Table 7 Estimated buckling loads and critical feeds for different work materials with tool of varying helix angles

S. no.	*Helix angle (degrees)*	*Buckling load (N)*	*Critical feeds (10^{-5} mm/rev)*			
		Proposed FE model (P_{cr})	*Aluminium*	*Carbon Steel*	*Stainless steel*	*alloy steel*
1	20	17.0	99.8	63.6	59.8	44.5
2	30	15.7	93.7	60.7	57.2	43.1
3	40	14.1	86.3	57	53.9	41.5
4	50	13.3	82.5	55.2	52.3	40.6

Figure 10 Effect of helix angle on the buckling load (see online version for colours)

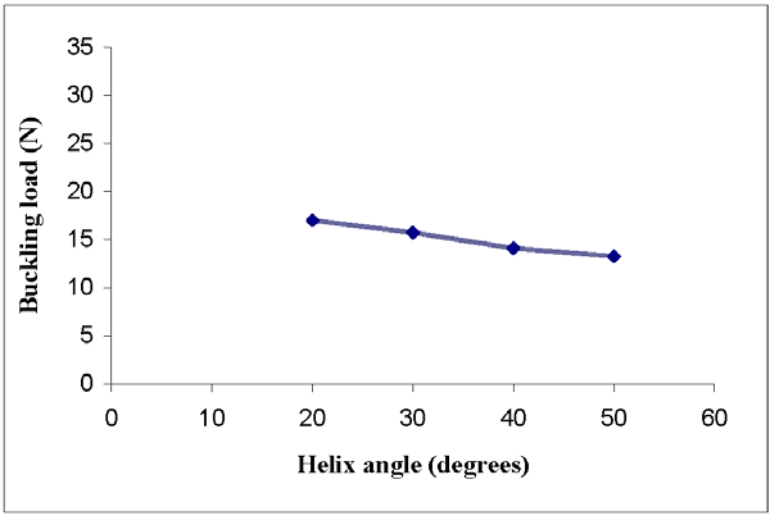

Figure 11 Effect of helix angle on the critical feed for different workpiece materials (see online version for colours)

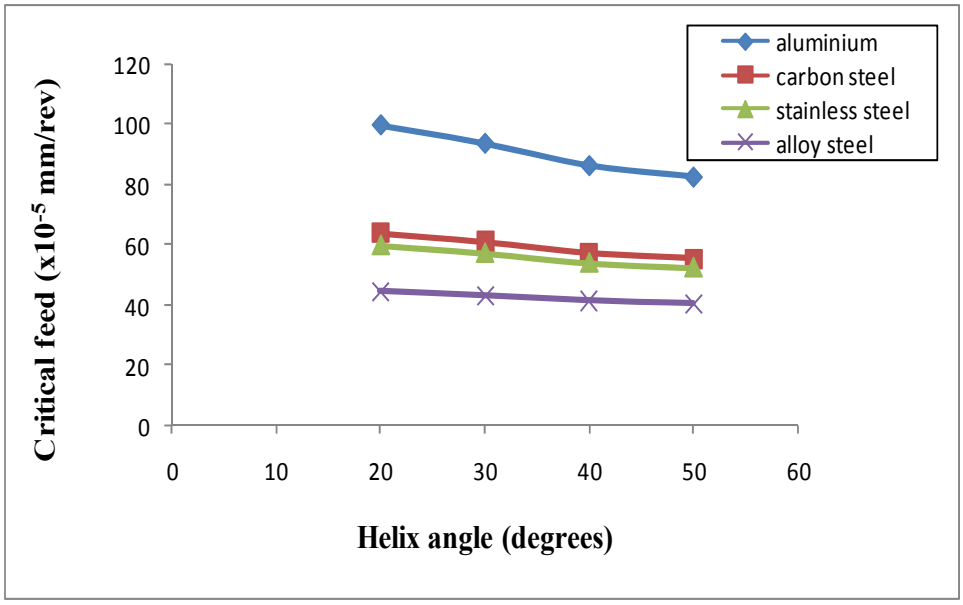

3.3.4 Variation with lip angle

The lip angle is varied in step of 10° and the buckling load, critical feed is determined for different tool materials with 40° Helix angle, 7 mm flute length and 0.5 mm diameter. The results are summarised in Table 8. It is found that influence of change in lip angle on the buckling load and critical feed of the drill bit is very insignificant as seen in Figure 12 and Figure 13. The variation of the critical feed with varying drill geometry for machining of various workpiece materials like aluminium, carbon steel, stainless steel and alloy steel is also insignificant as seen in Figure 13.

Table 8 Critical feed values for varying lip angle values with 40° Helix angle, 7 mm flute length and 0.5 mm diameter

S. no.	*Lip angle (degrees)*	*Buckling load (N)*	*Critical feeds (10^{-5} mm/rev)*			
		Proposed FE model (P_{cr})	*Aluminium*	*Carbon steel*	*Stainless steel*	*alloy steel*
1	80	16.22	96.0	61.8	58.2	43.6
2	90	16.05	95.2	61.4	57.8	43.5
3	100	15.96	94.8	61.2	57.6	43.4
4	110	15.84	94.2	60.9	57.4	43.2
5	120	15.73	93.7	60.7	57.2	43.1

Figure 12 Variation of buckling load with lip angle (see online version for colours)

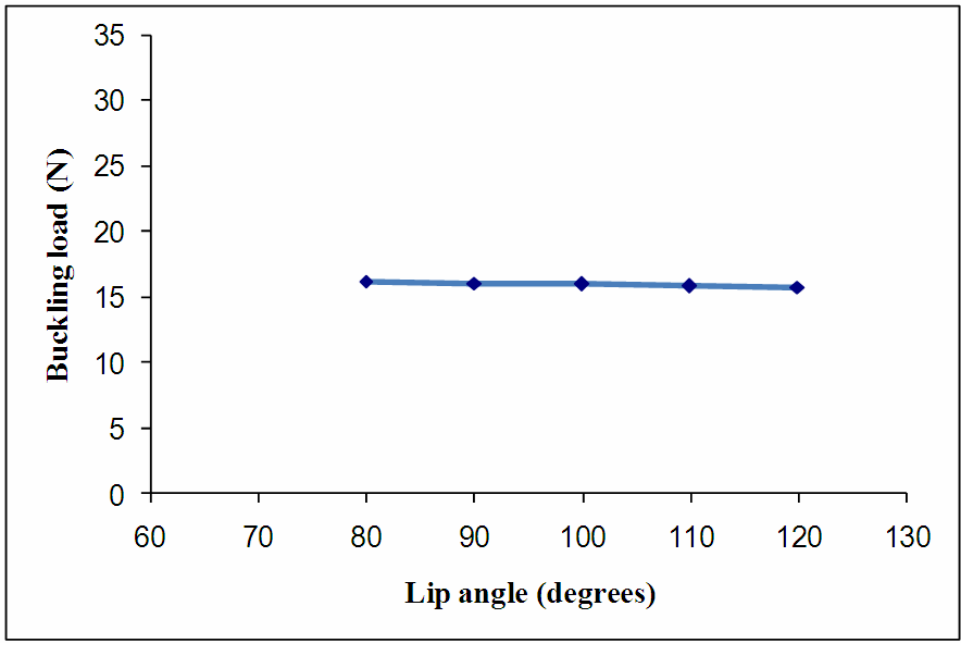

Figure 13 Effect of lip angle on the critical feed for different workpiece materials (see online version for colours)

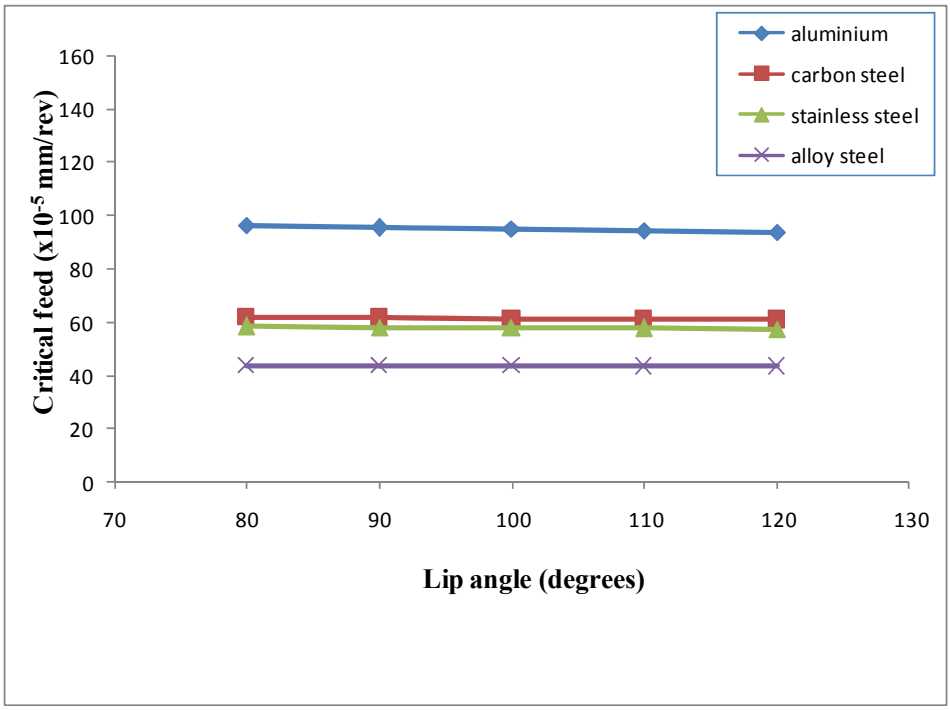

3.4 Modal analysis of microdrills

Modal analysis was performed to estimate different natural frequencies of vibrations corresponding to different mode shapes. The natural frequencies obtained from the modal analysis in ANSYS represent the critical speeds for the drill bits. Figure 14 shows the influence of various parameters, such as micro-drill diameter, flute length and helix angle on mode frequencies.

Figure 14(a) shows the plots of different modes and natural frequency corresponding to the drill diameters. For mode 1 and mode 2, values of modal frequencies decrease with increase in the drill diameter. Plots for mode 3 and mode 4 also shows similar trend in the values of the modal frequencies with smaller diameter drills. However, values of natural frequencies increase as the drill diameter increases from 0.3 to 0.4 mm. Subsequently, once again a decreasing trend in values of natural frequencies is observed with increase in the drill diameter. Yongping et al. (2003) have also reported that the effect of drill diameter on the modal frequency is complex. Figure 14(b) shows plots of different modes and natural frequencies corresponding to the flute length. Values of natural frequencies decrease with increase in the flute lengths. Similar trend was also observed by Yongping et al. (2003). Figure 14(c) shows plots of different modes and natural frequency corresponding to the helix angle. In this case, values of natural frequencies decrease with increase in the values of the helix angle. As a result of drill vibration, wandering motion is also likely to occur for a boundary condition where a lateral motion is possible due to a small axial force. That is there is not enough damping between the drill bit and the workpiece to stabilise the motion of a drill bit, which is typical during the initial phase of the drilling process resulting in a positional inaccuracy.

Figure 14 Influence of tool-geometry on modal frequencies (a) variation with drill diameter (b) variation with flute length (c) variation with helix angle (see online version for colours)

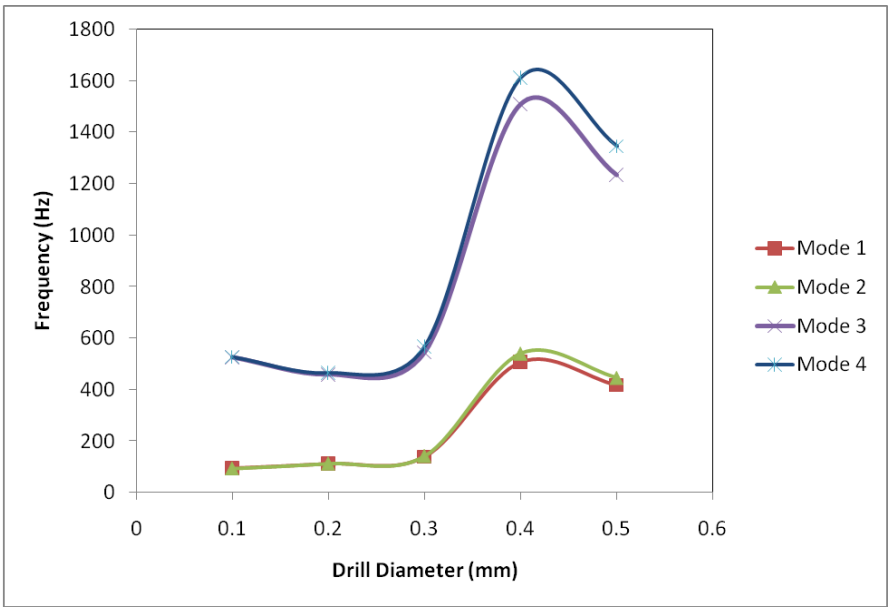

(a)

Figure 14 Influence of tool-geometry on modal frequencies (a) variation with drill diameter (b) variation with flute length (c) variation with helix angle (see online version for colours) (continued)

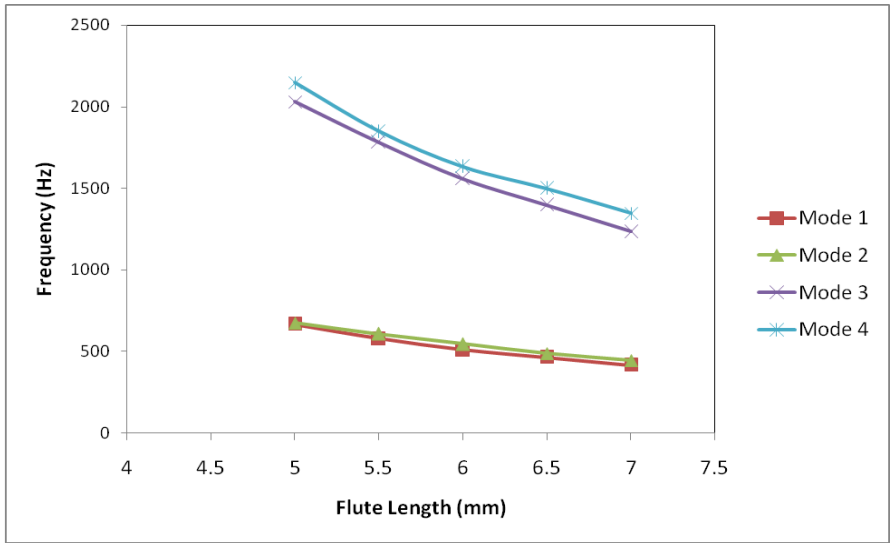

(b)

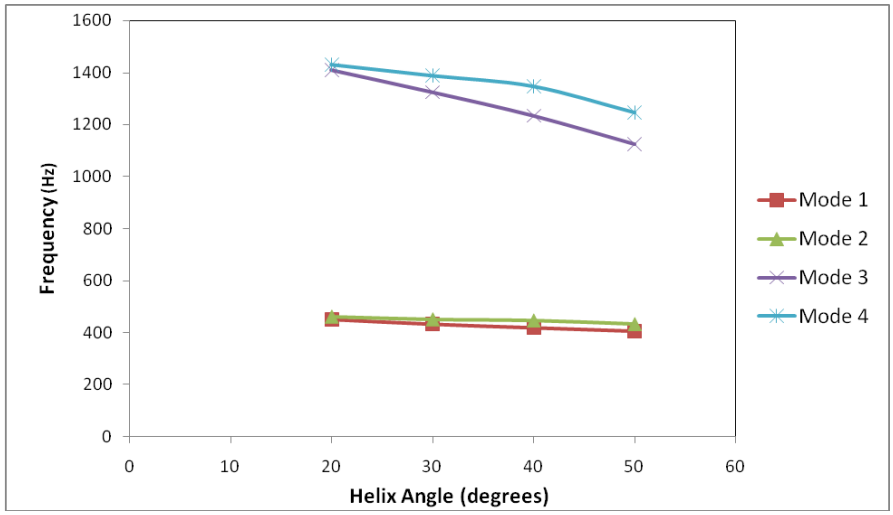

(c)

4 Conclusions

In the present work, finite element modelling approach combined with empirical analysis is used to determine critical speeds and feeds during microdrilling of various metals, such as aluminium, carbon steel, stainless-steel and alloy steel. The influence of different geometric parameters of drill bits on buckling load is investigated. Buckling loads

estimated using the finite model are compared and validated using Euler formula. It is found that proposed model closely follows the Euler formula. The stress distribution for the cutting edge and chisel edges of a typical microdrill were obtained for different loading conditions. During microdrilling the stress concentration is high at chisel edge and the cutting edges. The maximum stresses are at the region where chisel edge and cutting edge meet. Results obtained in the present study are qualitatively in agreement to that of the published results.

It is observed that the drill length and diameter significantly influences the buckling of microdrill. From the buckling analysis, the critical feed values were determined for the different work materials such as aluminium, carbon steel, stainless steel and alloy steel. The variation of critical feed for different drill geometry while machining various work materials is analysed. The study indicates that for harder materials, like steels, feed is a critical parameter and should be lower as compared to other soft materials, to avoid breakage of the tools. The proposed approach will help in deciding the operating parameters based on the critical feeds. It is also useful in simulating the wandering motion of the drills during the initial phase and determining the positional accuracy of the micro features.

References

Chen, W.R. (2007) 'Parametric studies on buckling loads and critical speeds of microdrill bits', *International Journal of Mechanical Sciences*, Vol. 49, pp.935–949.

Chen, W.S. and Ehmann, K.F. (1994) 'An experimental investigation on the wear and performance of micro-drills', *Tribology in Manufacturing, Proc. of ASME, TRIB*, Vol. 5, pp.145–157.

Cheong, M.S., Cho, D.W. and Ehmann, K.F. (1999) 'Identification and control for micro drill productivity enhancement', *International Journal of Machine Tools and Manufacture*, Vol. 39, pp.1539–1561.

Chyan, H.C. and Ehmann, K.F. (1998) 'Development of curved helical micro drill technology for micro-hole drilling', *Mechatronics*, Vol. 8, pp.337–358.

Fu, L., Ling, S.F. and Tseng, C.H. (2007) 'On-line breakage monitoring of small drills with input impedance of driving motor', *Mechanical Systems and Signal Processing*, Vol. 2, pp.457–465.

Gurkan, S. and Mustafa, S. (2004) 'Buckling and dynamic stability of a rotating pre-twisted asymmetric cross-section blade subjected to an axial periodic force', *Finite Elements in Analysis and Design*, Vol. 40, pp.1399–1415.

Hinds, B.K. and Treanor, G.M. (2000) 'Analysis of stresses in micro-drills using the finite element method', *International Journal of Machine Tools and Manufacture*, Vol. 40, pp.1443–1456.

Jeong, Y.H. and Min, B.K. (2007) 'Geometry prediction of EDM drilled holes and tool electrode shapes of micro EDM process using simulation', *International Journal of Machine Tools and Manufacture*, Vol. 47, pp.1817–1826.

Joseph, M.G. (2002) *Micro Machining of Engineering Materials*, Dekker, New York.

Jung, F.H. (2005) 'Mathematical model for helical drill point', *International Journal of Machine Tools and Manufacture*, Vol. 45, pp.967–977.

Kim, D.W., Lee, Y.S., Park, M.S. and Chu, C.N. (2009) 'Tool life improvement by peck drilling and thrust force monitoring during deep-micro-hole drilling of steel', *International Journal of Machine Tools and Manufacture*, Vol. 49, pp.246–355.

Mahalik, N.P. (2006) *Micro Manufacturing and Nanotechnology*, Springer, New York.

Pei, Y., Tan, Q. and Yang, Z. (2006) 'A study of dynamic stresses in micro drills under high-speed machining', *International Journal of Machine Tools and Manufacture*, Vol. 46, pp.1892–1900.

Rahman, A.A., Mamat, A. and Wagiman, A. (2009) 'Effect of machining parameters on hole quality of micro drilling for brass', *Modern Applied Science*, Vol. 3, No. 5, pp.221–230.

Sedat, K. (2007) 'Analysis of drill dynamometer with octagonal ring transducers for monitoring of cutting forces in drilling', *Materials and Design*, Vol. 28, pp.673–685.

Strenkowski, J.S., Hsieh, C.C. and Shih, A.J. (2004) 'An analytical finite element technique for predicting thrust force and torque in drilling', *International Journal of Machine Tools and Manufacture*, Vol. 44, pp.1413–1421.

Sunil, K.S. (2007) 'Combined torsional bending axial dynamics of a twisted rotating cantilever timoshenko beam with contact impact loads at the free-end', *Journal of Applied Mechanics*, Vol. 74, pp.505–522.

Watanabe, H., Tsuzaka, H. and Masuda, M. (2008) 'Micro-drilling for printed circuit boards (PCBs) – influence of radial run-out of micro drills on hole quality', *Precision Engineering*, Vol. 32, pp.329–335.

Yongping, G., Ehmann, K.F. and Cheng, L. (2003) 'Analysis of dynamic characteristics of micro drills', *Journal of Materials Processing Technology*, Vol. 141, pp.16–28.

Nomenclature

Symbol	*Description*	*Unit*
A	Area of cross-section	mm^2
d	diameter	mm
E	The Young's modulus	GPa
f	feed rate	mm/rev
G	shear modulus	GPa
H	Brinell hardness of the workpiece	$Kg\text{-}f/mm^2$
I	Moment of inertia of the element	$kg\text{-}mm^2$
Ip	Polar moment of inertia	mm^4
K	Specific cutting force	N/mm^2
k	Poisson's ratio	-
M	Torque	N-mm
P	Axial load/force	N
T	Thrust force	N
t	Time	sec
U	Potential Energy	J
K_B	Stiffness matrix due to bending and shear effects	-
K_F	Stiffness matrix due to axial force	-
K_W	Stiffness matrix due to rotational speed	-
$[C]$	Damping matrix of the system	-
ω	Rotational velocity of the system	rad/sec
θ_x, θ_y	Angular displacements in x, y directions	radians
ρ	Density	kg/mm^3